

## Article

# New Hygrocins K–U and Streptophenylpropanamide A and Bioactive Compounds from the Marine-Associated *Streptomyces* sp. ZZ1956

Wenwen Yi <sup>1</sup>, Asif Wares Newaz <sup>1</sup>, Kuo Yong <sup>1</sup>, Mingzhu Ma <sup>1,2</sup>, Xiao-Yuan Lian <sup>3,\*</sup> and Zhizhen Zhang <sup>1,\*</sup> <sup>1</sup> Ocean College, Zhoushan Campus, Zhejiang University, Zhoushan 316021, China<sup>2</sup> Zhejiang Marine Development Research Institute, Zhoushan 316000, China<sup>3</sup> College of Pharmaceutical Sciences, Zhejiang University, Hangzhou 310058, China

\* Correspondence: xylian@zju.edu.cn (X.-Y.L.); zzhang88@zju.edu.cn (Z.Z.); Tel.: +86-13675859706 (Z.Z.)

**Abstract:** Marine-derived *Streptomyces* actinomycetes are one of the most important sources for the discovery of novel bioactive natural products. This study characterized the isolation, structural elucidation and biological activity evaluation of thirty compounds, including twelve previously undescribed compounds, namely hygrocins K–U (5–13, 17 and 18) and streptophenylpropanamide A (23), from the marine-associated actinomycete *Streptomyces* sp. ZZ1956. Structures of the isolated compounds were determined by a combination of extensive NMR spectroscopic analyses, HRESIMS data, the Mosher's method, ECD calculations, single crystal X-ray diffraction and comparison with reported data. Hygrocins C (1), D (2), F (4), N (8), Q (11) and R (12), 2-acetamide-6-hydroxy-7-methyl-1,4-naphthoquinone (22), echoside C (27), echoside A (28) and 11,11'-*O*-dimethylelaiophylin (30) had antiproliferative activity (IC<sub>50</sub>: 0.16–19.39 μM) against both human glioma U87MG and U251 cells with hygrocin C as the strongest active compound (IC<sub>50</sub>: 0.16 and 0.35 μM, respectively). The analysis of the structure–activity relationship indicated that a small change in the structures of the naphthalenic ansamycins had significant influence on their antiglioma activities. Hygrocins N (8), O (9), R (12), T (17) and U (18), 2-amino-6-hydroxy-7-methyl-1,4-naphthoquinone (21), 2-acetamide-6-hydroxy-7-methyl-1,4-naphthoquinone (22), 3'-methoxy(1,1',4',1''-terphenyl)-2',6'-diol (26), echoside C (27) and echoside A (28) showed antibacterial activity against methicillin-resistant *Staphylococcus aureus* and *Escherichia coli* with MIC values of 3–48 μg/mL.

**Keywords:** marine *Streptomyces* sp. ZZ1956; Streptomycetaceae; hygrocins K–U; streptophenylpropanamide A; structure elucidation; antiglioma activity; antibacterial activity



**Citation:** Yi, W.; Newaz, A.W.; Yong, K.; Ma, M.; Lian, X.-Y.; Zhang, Z.

New Hygrocins K–U and Streptophenylpropanamide A and Bioactive Compounds from the Marine-Associated *Streptomyces* sp. ZZ1956. *Antibiotics* **2022**, *11*, 1455.

<https://doi.org/10.3390/antibiotics11111455>

Academic Editors: Zeinab Khalil and Marcelo Marucci Pereira Tangerina

Received: 1 October 2022

Accepted: 21 October 2022

Published: 22 October 2022

**Publisher's Note:** MDPI stays neutral with regard to jurisdictional claims in published maps and institutional affiliations.



**Copyright:** © 2022 by the authors. Licensee MDPI, Basel, Switzerland. This article is an open access article distributed under the terms and conditions of the Creative Commons Attribution (CC BY) license (<https://creativecommons.org/licenses/by/4.0/>).

## 1. Introduction

Compound 3-amino-5-hydroxy benzoic acid (3,5-AHBA) is the precursor of a big group of natural products, including the ansamycins, the mitomycins and the unique saliniketals (degraded ansamycins) [1]. The ansamycins have two characteristic structural features: an aromatic core and a so-called ansa bridge containing a lactam moiety, whose two ends link to two nonadjacent positions of the aromatic core [2]. The ansamycins can be divided into naphthalenic or benzenic depending on the nature of their aromatic ring. The naphthalenic ansamycins include rifamycins, ansalactams, chaxamycins, divergolides, hygrocins, naphthomycins, rubradirins and streptovaricins. Their structural characteristic is a 1,4-naphthoquinone or a 1,4-hydroxynaphthalene chromophore. Benzenic ansamycins have a 1,4-benzoquinone or a 1,4-hydrobenzoquinone chromophore and include ansatrienins, cebulactams, cytotrienins, geldanamycins, herbimycins, macbecins, maytansines (ansamitocins) and tetrapetalones. Precursor feeding experiments and genetic and biochemical methods have been applied to investigate the biosynthesis of the ansamycins, demonstrating that AHBA is the source of the chromophore and the aliphatic ansa chains are derived from acetate, propionate, isobutyrate or glycolate units [1,2].

While most of the ansamycins were isolated from actinomycetes, the class of maytansines was also found in higher plants and mosses [3,4]. However, the first maytansines found in plants [4] are now known to be produced by the interplay amongst bacteria in the root system [5]. It was reported that nearly 300 ansamycins have been identified from natural sources [6] and more and more ansamycins continue to be reported, such as the recently described olimycins from the *ovmO*-inactivated mutant strain *Streptomyces olivaceus* SCSIO T05 [7] and ansaseomycins from a heterologous mutant strain of *Streptomyces seoulensis* [8]. The ansamycins exhibit diverse biological activities, such as antibacterial (naphthomycin A, rifamycin, rubradirin and streptovaricin A), anticancer (ansamitocins P-3, ansatrienins A, geldanamycin, mitomycin C, saliniketals A and B), lipoxygenase inhibitory (tetrapetalones A and B) and antiviral (divergolide O) activities [1,9]. The well-known drugs of the ansamycin family were the first-line anti-tuberculous drug rifamycin and the antibody–drug conjugate Kadcyra (emtansine).

As part of an ongoing project to discover novel antiglioma natural products from marine microorganisms [10–20], we isolated an actinomycete from a sediment sample collected from an intertidal mangrove area at the Pacific Ocean close to South Sulawesi, Indonesia. This actinomycete was assigned as *Streptomyces* sp. ZZ1956 based on its 16S rDNA sequence analysis (Figure S1 and Table S1). An extract prepared from the culture of the strain ZZ1956 in GYM liquid medium exhibited inhibitory activity against the proliferation of glioma U251 and U87MG cells with inhibition rates of over 90%. Chemical investigation of this active extract resulted in the isolation and identification of thirty compounds 1–30, including eleven new naphthalenic ansamycin analogues hygrocins K–U (5–13, 17, 18) and one new phenylpropanamide derivative streptophenylpropanamide A (23) (Figure 1). Herein, we described the isolation and culture of the strain ZZ1956 as well as the isolation, structure elucidation and bioactive evaluation of these isolated compounds.

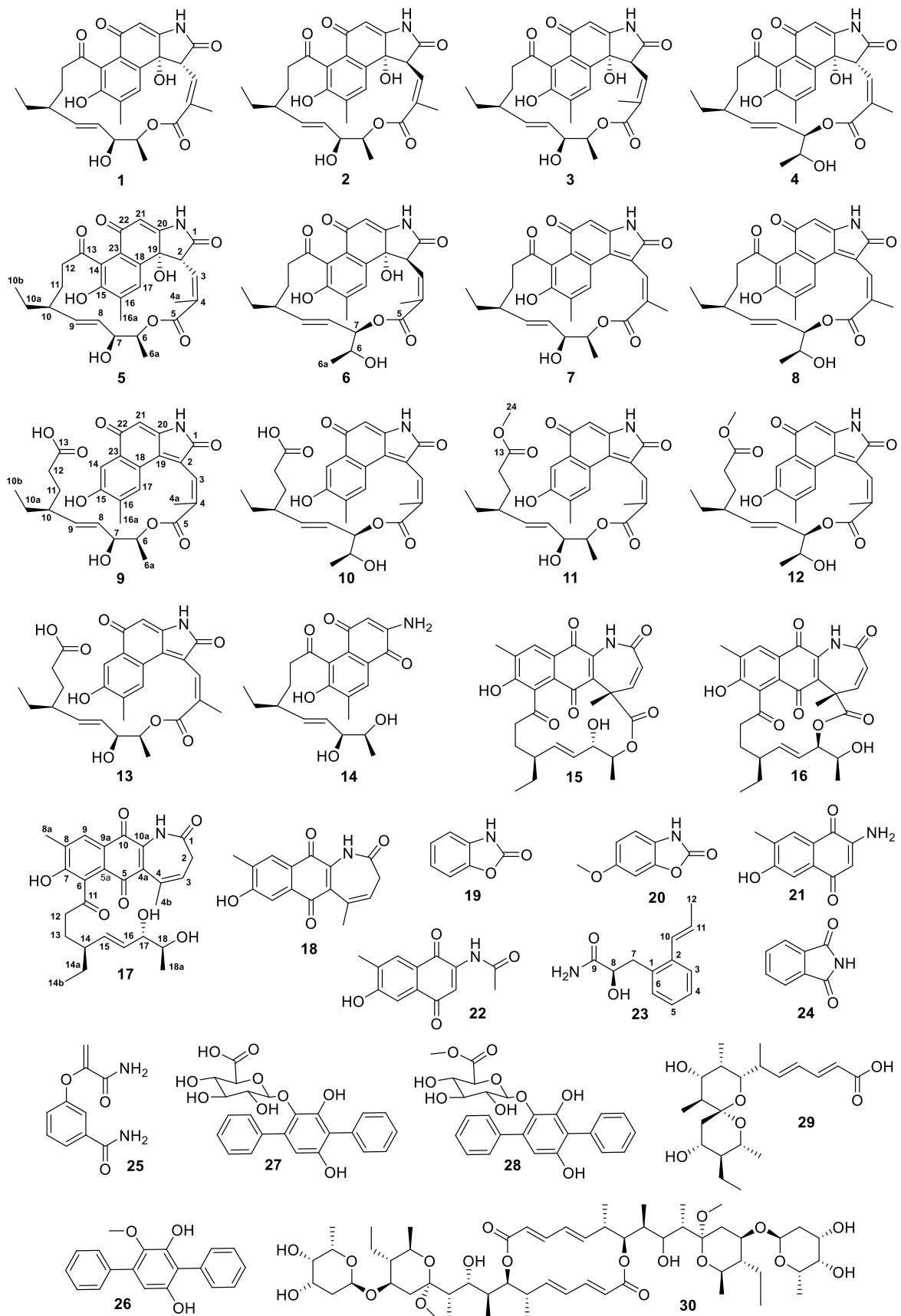


Figure 1. Structure of isolated compounds 1–30.

## 2. Results and Discussion

### 2.1. Structure Elucidation of the Isolated Compounds

After analyses of the NMR spectroscopic data and comparison with related data of references, eighteen known compounds were elucidated to be hygrocins C–F (1–4) [21], degra-hygrocin A (14) [22], hygrocins B (15) [22], hygrocins G (16) [21], benzoxazolone (19) [23], coixol (20) [24], 2-amino-6-hydroxy-7-methyl-1,4-naphthoquinone (21) [25], 2-acetamide-6-hydroxy-7-methyl-1,4-naphthoquinone (22) [26], 1H-isoindole-1,3(2H)-dione (24) [27], 3-(3'-amino-3'-oxoprop-1'-en-2'-yl)oxy benzamide (25) [28], 3'-methoxy(1,1',4',1''-terphenyl)-2',6'-diol (26) [29], echoside C (27) [30], echoside A (28) [30], pteridic acid hydrate (29) [31] and 11,11'-O-dimethylelaioaphyllin (30) [32]. The structure of hygrocins C (1) was confirmed by single crystal X-ray diffraction (Table S2). Degrathygrocin A (14) was previously reported as an alkaline hydrolytic product of hygrocins A [22]; while 2-acetamide-6-hydroxy-7-methyl-1,4-naphthoquinone (22) was an intermediate compound of chemical synthesis of ansalactam A [26]. Therefore, both compounds 14 and 22 are reported as natural products for the first time. The NMR data of these known compounds are presented in Tables S3–S14.

Compound 5 had the same molecular formula  $C_{28}H_{31}NO_8$  and very similar UV characteristic absorptions as hygrocins C–F (1–4), indicating that they are isomers. Careful analyses of the  $^1H$ ,  $^{13}C$ , HMQC, COSY, HMBC and NOESY NMR spectra of 5 demonstrated that its structure was different from those of 1–4 in the configurations at C-2 and C<sub>3</sub>–C<sub>4</sub> double bond as well as the position of the lactone ring formation. The configuration at C-2 was established as *R* based on a strong NOE correlation observed between H-2 and H<sub>3</sub>-6a (Figure 2). A strong NOE correlation of H-2 with H<sub>3</sub>-6a was an indication of 2*R*-configuration in 1 and 4, compared to the 2*S*-configuration in 2 and 3 without the NOE correlation of H-2 and H<sub>3</sub>-6a [21]. The chemical shift value ( $\delta_C$  13.7) of C-4a in 5 indicated a 3*E*-configuration, compared to the downfield chemical shift values ( $\delta_C$  21.1–22.2) (Tables S3 and S4) of C-4a for a 3*Z*-configuration in 1, 2 and 4 [21]. Observed strong NOE (for 7, 8, 13), no NOE (for 10–12) or weak NOE (5, 6, 9) correlation between H-3 and H<sub>3</sub>-4a also supported the assignment of the 3*E*- or 3*Z*-configuration. In addition, the *trans*-coupling constant value of 16.0 Hz ( $^3J_{H8/H9}$ ) indicated an 8*E*-configuration and the small vicinal coupling constant value of 2.8 Hz ( $^3J_{H6/H7}$ ) suggested a *syn* orientation between H-6 and H-7 [21]. HMBC correlations (Figure 2) of H-6 ( $\delta_H$  4.65) with C-5 ( $\delta_C$  167.7) established the linkage of C<sub>5</sub> and C<sub>6</sub> through an oxygen to form the lactone ring. It is known that hygrocins C–E (1–3) have the same 6*S*, 7*S*, 10*S*, 19*R*-configuration. Therefore, we proposed compound 5 to have the same 6*S*, 7*S*, 10*S*, 19*R*-configuration as 1–3 based on a common biosynthetic origin. Based on the above analyses, it can be concluded that the structure of 5 is similar to that of 1 with the only difference being the configuration of the C<sub>3</sub>–C<sub>4</sub> double bond. Therefore, the structure of 5 was elucidated as a previously undescribed member of the naphthoquinone ansamycins, named hygrocins K. Its  $^{13}C$  and  $^1H$  NMR data are reported in Tables 1 and 2.

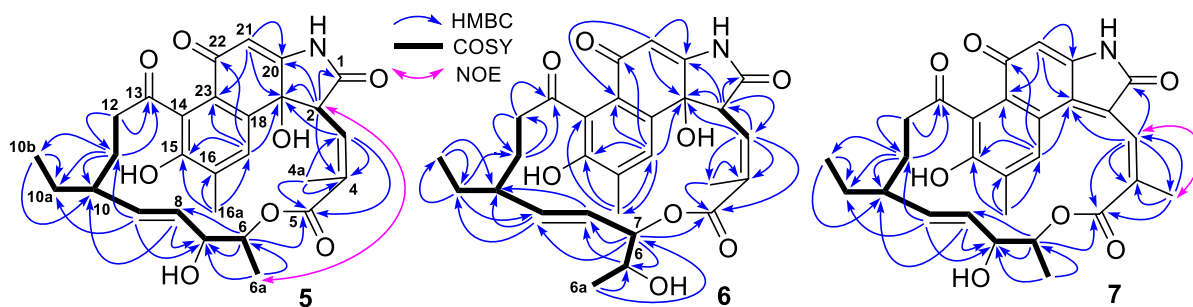


Figure 2. COSY, key HMBC and NOE correlations of hygrocins K–M (5–7).

**Table 1.**  $^{13}\text{C}$  NMR data of compounds 5–13 (150 MHz, in MeOH- $d_4$ ,  $\delta_{\text{C}}$ ).

No.	5	6	7	8	9	10	11	12	13
1	177.3, C	177.1, C	172.5, C	173.1, C	171.6, C	171.6, C	171.5, C	171.7, C	171.7, C
2	56.9, CH	56.9, CH	121.9, C	122.6, C	126.8, C	126.8, C	126.8, C	126.8, C	126.6, C
3	133.1, CH	133.6, CH	128.9, CH	127.5, CH	129.7, CH	129.7, CH	129.7, CH	129.7, CH	129.7, C
4	133.9, C	133.5, C	137.5, C	137.8, C	137.6 <sup>a</sup> , C	137.7 <sup>a</sup> , C	137.6 <sup>a</sup> , C	137.7 <sup>a</sup> , C	138.3, C
4a	13.7, CH <sub>3</sub>	13.6, CH <sub>3</sub>	21.1, CH <sub>3</sub>	22.1, CH <sub>3</sub>	16.4, CH <sub>3</sub>	16.4, CH <sub>3</sub>	16.4, CH <sub>3</sub>	16.4, CH <sub>3</sub>	21.1, CH <sub>3</sub>
5	167.7, C	167.3, C	167.6, C	168.3, C	168.1, C	167.9, C	168.1, C	167.9, C	168.5, C
6	75.3, CH	69.5, CH	74.7, CH	68.5, CH	75.6, CH	69.9, CH	75.5, CH	69.9, CH	75.2, CH
6a	15.2, CH <sub>3</sub>	19.1, CH <sub>3</sub>	13.5, CH <sub>3</sub>	19.1, CH <sub>3</sub>	16.4, CH <sub>3</sub>	19.6, CH <sub>3</sub>	16.2, CH <sub>3</sub>	19.6, CH <sub>3</sub>	15.0, CH <sub>3</sub>
7	74.2, CH	77.9, CH	71.3, CH	80.6, CH	75.4, CH	81.4, CH	75.3, CH	81.2, CH	74.4, CH
8	128.2, CH	125.3, CH	128.7, CH	124.4, CH	131.5, CH	127.9, CH	131.5, CH	127.9, CH	130.7, CH
9	138.3, CH	136.5, CH	137.3, CH	139.9, CH	138.3, CH	141.3, CH	138.1, CH	140.9, CH	137.9, CH
10	41.9, CH	41.9, CH	43.8, CH	43.4, CH	45.6, CH	45.8, CH	45.6, CH	45.8, CH	45.5, CH
10a	26.3, CH <sub>2</sub>	26.6, CH <sub>2</sub>	26.6, CH <sub>2</sub>	29.2, CH <sub>2</sub>	29.2, CH <sub>2</sub>	29.1, CH <sub>2</sub>	29.2, CH <sub>2</sub>	29.1, CH <sub>2</sub>	29.1, CH <sub>2</sub>
10b	10.6, CH <sub>3</sub>	12.4, CH <sub>3</sub>	12.7, CH <sub>3</sub>	11.5, CH <sub>3</sub>	12.3, CH <sub>3</sub>	12.3, CH <sub>3</sub>	12.3, CH <sub>3</sub>	12.3, CH <sub>3</sub>	12.2, CH <sub>3</sub>
11	29.2, CH <sub>2</sub>	33.0, CH <sub>2</sub>	32.1, CH <sub>2</sub>	28.9, CH <sub>2</sub>	31.1, CH <sub>2</sub>	31.2, CH <sub>2</sub>	31.0, CH <sub>2</sub>	31.0, CH <sub>2</sub>	30.9, CH <sub>2</sub>
12	41.8, CH <sub>2</sub>	42.2, CH <sub>2</sub>	39.4, CH <sub>2</sub>	42.5, CH <sub>2</sub>	33.0, CH <sub>2</sub>	33.2, CH <sub>2</sub>	33.0, CH <sub>2</sub>	33.0, CH <sub>2</sub>	33.0, CH <sub>2</sub>
13	212.0, C	211.2, C	212.9, C	212.0, C	177.7, C	177.8, C	176.0, C	176.0, C	177.7, C
14	130.1, C	127.2, C	129.9, C	129.2, C	113.9, CH	113.9, CH	113.9, CH	113.9, CH	113.7, CH
15	153.0, C	153.7, C	158.7, C	158.0, C	159.8, C	159.8, C	159.9, C	159.9, C	159.5, C
16	133.1 <sup>a</sup> , C	133.4, C	133.3, C	133.7, C	131.9 <sup>b</sup> , C	131.9, C	131.9, C	131.9, C	132.2, C
16a	17.0, CH <sub>3</sub>	16.9, CH <sub>3</sub>	17.3, CH <sub>3</sub>	17.2, CH <sub>3</sub>	16.8, CH <sub>3</sub>	16.8, CH <sub>3</sub>	16.8, CH <sub>3</sub>	16.8, CH <sub>3</sub>	16.7, CH <sub>3</sub>
17	131.5, CH	132.1, CH	131.3, CH	130.7, CH	131.7 <sup>b</sup> , CH	131.6, CH	131.6, CH	131.6, CH	131.7, CH
18	133.0 <sup>a</sup> , C	134.0, C	131.2, C	130.1, C	122.8, C	122.8, C	122.7, C	122.8, C	123.2, C
19	75.4, C	75.8, C	134.8, C	136.4, C	137.4 <sup>a</sup> , C	137.4 <sup>a</sup> , C	137.4 <sup>a</sup> , C	137.4 <sup>a</sup> , C	139.6, C
20	164.6, C	164.5, C	154.8, C	155.1, C	154.0, C	154.0, C	154.0, C	154.0, C	154.5, C
21	105.1, CH	105.3, CH	106.0, CH	105.8, CH	106.3, CH	106.4, CH	106.3, CH	106.4, CH	106.0, CH
22	185.6, C	185.9, C	187.4, C	187.0, C	186.5, C	186.4, C	186.4, C	186.4, C	186.7, C
23	129.7, C	131.1, C	129.3, C	128.4, C	131.9 <sup>b</sup> , C	131.9, C	131.9, C	131.9, C	131.7, C
24	-	-	-	-	-	-	52.1, CH <sub>3</sub>	52.2, CH <sub>3</sub>	-

<sup>a,b</sup> The data with the same labels in each column may be interchanged.**Table 2.**  $^1\text{H}$  NMR data of compounds 5–8 (600 MHz, in MeOH- $d_4$ ,  $\delta_{\text{H}}$ , multi.,  $J$  in Hz).

No.	5	6	7	8
2	4.06, d (11.1)	4.04, d (11.1)	-	-
3	6.09, dd (11.1, 1.8)	6.10, dd (11.1, 1.4)	6.90, s	6.81, s
4a	2.06, d (1.8)	2.03, s	2.21, s	2.19, s
6	4.65, m	3.67, m	4.87 <sup>a</sup> , m	3.69, m
6a	1.15, d (6.4)	1.02, d (6.7)	0.91, d (6.0)	0.95, d (6.4)
7	3.90, dd (6.8, 2.8)	5.11, t (5.0)	3.86, m	4.97, t (5.8)
8	4.92, dd (16.0, 6.8)	5.26, dd (16.1, 5.0)	4.59, d (15.1)	4.41, dd (15.6, 6.6)
9	5.50, dd (16.0, 5.5)	5.06, dd (16.1, 6.4)	5.30, dd (15.1, 9.2)	5.36, dd (15.6, 5.8)
10	1.84, m	1.69, m	1.55, m	1.56, m
10a	1.49, m; 1.23, m	1.32, m	1.48, m; 0.92, m	1.30, m; 1.14, m
10b	0.71, t (7.3)	0.82, t (7.4)	0.69, t (7.2)	0.76, t (7.2)
11	1.45, m; 1.19, m	1.55, m; 1.38, m	1.28, m; 1.18, m	1.53, m; 1.35, m
12	2.71, m; 2.59, m	2.67, m; 2.49, m	2.75, d (11.6)	2.81, dd (16.8, 8.5); 2.43, dd (16.8, 10.0)
16a	2.29, s	2.27, s	2.21, s	2.15, s
17	7.22, s	7.28, s	7.57, s	7.65, s
21	5.87, s	5.93, s	5.85, s	5.81, s

<sup>a</sup> The data was overlapped with that of H<sub>2</sub>O.

Compound **6** had the same molecular formula C<sub>28</sub>H<sub>31</sub>NO<sub>8</sub> as **1–5** deduced from its HRESIMS ion peak at  $m/z$  508.1979 [M-H]<sup>-</sup> and  $^{13}\text{C}$  NMR data. Careful analyses of its 1D- and 2D-NMR spectra determined that **6** and hygrocins F (**4**) had the same planar structure.



H<sub>3</sub>-4a in **9** or **10** indicated a 3*E*-configuration, compared to the downfield shift values at  $\delta_C$  21.1 and 22.1 (Table 1) for the C-4a and the strong NOE correlation between H-3 and H<sub>3</sub>-4a in **7** and **8** with a 3*Z*-configuration. Therefore, the structures of **9** and **10** were elucidated as two previously reported naphthoquinone ansamycins, named hygrocins O (**9**) and hygrocins P (**10**). Their <sup>13</sup>C and <sup>1</sup>H NMR data are reported in Tables 1 and 3.

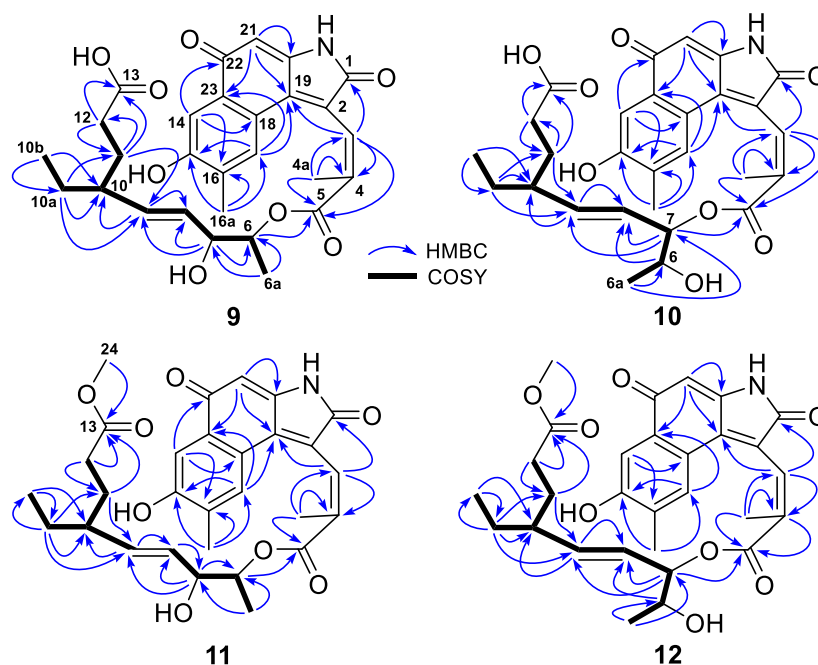


**Figure 4.** COSY and key HMBC correlations of hygrocins O–R (**9**–**12**).

**Table 3.** <sup>1</sup>H NMR data of compounds **9**–**13** (600 MHz, in MeOH-*d*<sub>4</sub>,  $\delta_H$ , multi., *J* in Hz).

No.	<b>9</b>	<b>10</b>	<b>11</b>	<b>12</b>	<b>13</b>
3	7.53, s	7.54, s	7.51, s	7.54, d (1.4)	7.54, s
4a	1.92, s	1.92, s	1.92, s	1.93, d (1.4)	2.24, s
6	5.05, m	3.93, m	5.06, m	3.92, m	4.84, m
6a	1.34, d (6.4)	1.24, d (6.6)	1.33, d (6.4)	1.24, d (6.4)	1.14, d (6.4)
7	4.19, t (6.3)	5.23, t (6.6)	4.19, t (6.1)	5.24, t (6.3)	4.03, t (6.0)
8	5.54, dd (15.5, 6.3)	5.57, m	5.52, dd (15.5, 6.1)	5.56, m	5.30, dd (15.5, 6.0)
9	5.48, dd (15.5, 8.6)	5.57, m	5.45, dd (15.5, 8.6)	5.57, m	5.24, dd (15.5, 8.8)
10	1.95, m	1.95, m	1.90, m	1.96, m	1.71, m
10a	1.43, m; 1.28, m	1.49, m; 1.31, m	1.45, m; 1.26, m	1.48, m; 1.29, m	1.26, m; 1.18, m
10b	0.87, t (7.1)	0.86, t (7.3)	0.86, t (7.2)	0.86, t (7.4)	0.76, t (7.4)
11	1.74, m; 1.46, m	1.76, m; 1.47, m	1.72, m; 1.41, m	1.77, m; 1.52, m	1.57, m; 1.09, m
12	2.30, m; 2.21, m	2.30, m; 2.23, m	2.28, m; 2.24, m	2.30, m; 2.26, m	2.10, m; 2.02, m
14	7.43, s	7.42, s	7.43, s	7.43, s	7.46, s
16a	2.24, s	2.21, s	2.23, s	2.21, s	2.28, s
17	7.42, s	7.39, s	7.40, s	7.40, s	6.83, s
21	5.88, s	5.88, s	5.87, s	5.88, s	5.88, s
24	-	-	3.57, s	3.65, s	-

Compounds **11** and **12** were also obtained as a red amorphous powder and had same molecular formula C<sub>29</sub>H<sub>33</sub>NO<sub>8</sub> deduced from their <sup>13</sup>C NMR data and HRESIMS ion peaks at *m/z* 522.2125 [M–H]<sup>–</sup> in **11** and 522.2132 [M–H]<sup>–</sup> in **12**, 14 mass units higher than those of **9** and **10**. Compared to the <sup>13</sup>C and <sup>1</sup>H NMR data of **9** and **10**, both **11** and **12** had additional NMR signals for a methoxy group at  $\delta_C$  52.1 and  $\delta_H$  3.57 (3H, s) in **11** and  $\delta_C$  52.2 and  $\delta_H$  3.65 (3H, s) in **12**. A HMBC correlation of H<sub>3</sub>-24 ( $\delta_H$  3.57) with C-13 ( $\delta_C$  176.0) in **11** and H<sub>3</sub>-24 ( $\delta_H$  3.65) with C-13 ( $\delta_C$  176.0) in **12** established the position of the

methoxy group. Further analyses of their HMQC, COSY, HMBC and NOE correlations (Figure 4) demonstrated that **11** and **12** were the methyl esters of **9** and **10**, respectively. The structures of **11** and **12** were thus identified as two previously undescribed naphthoquinone ansamycins, named hygrocin Q (**11**) and R (**12**). The  $^{13}\text{C}$  and  $^1\text{H}$  NMR data of **11** and **12** are reported in Tables 1 and 3. It should be noted that **11** and **12** may be the artificial products of methyl esterification of **9** and **10**, respectively, originated in the extraction and separation process.

The HRESIMS spectrum of compound **13** gave an ion peak at  $m/z$  508.1975  $[\text{M}-\text{H}]^-$ , corresponding to a molecular formula  $\text{C}_{28}\text{H}_{31}\text{NO}_8$ , which was the same as those of **9** and **10**. Detailed analyses of the 1D- and 2D-NMR spectra of **13** determined that **9** and **13** had the same planar structure and their structural difference was only the different configuration of the  $\text{C}_3\text{-C}_4$  double bond. The downfield shift value at  $\delta_{\text{C}}$  21.1 for C-4a and a strong NOE correlation between H-3 and H<sub>3</sub>-4a (Figure 5) suggested a 3*Z*-configuration in **13**. The structure of **13** was thus assigned as a previously undescribed naphthoquinone ansamycin, named hygrocin S (**13**). Its  $^{13}\text{C}$  and  $^1\text{H}$  NMR data (Tables 1 and 3) were assigned based on the HMQC, COSY and HMBC correlations (Figure 5).

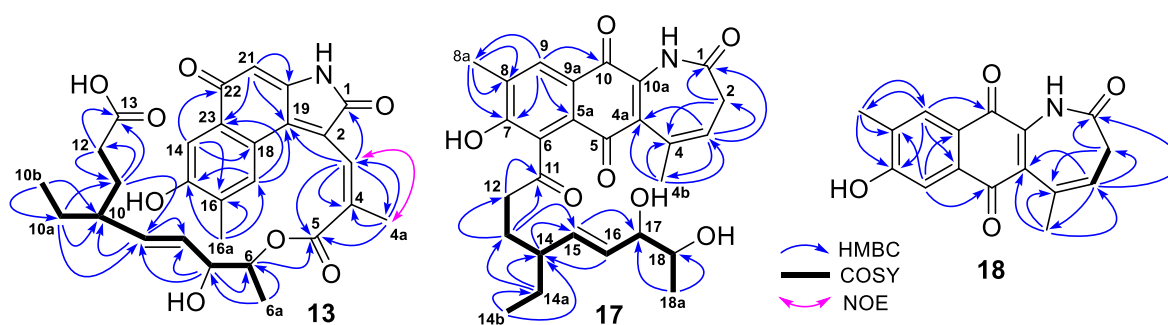


**Figure 5.** COSY and key HMBC correlations of hygrocins S–U (**13**, **17**, **18**).

Compound **17** was obtained as a yellow amorphous powder and its molecular formula  $\text{C}_{27}\text{H}_{31}\text{NO}_7$  was determined based on the HRESIMS ion peak at  $m/z$  480.2024  $[\text{M}-\text{H}]^-$  and  $^{13}\text{C}$  NMR data. Interpretation of the  $^1\text{H}$ ,  $^{13}\text{C}$  and HMQC NMR spectra of **17** indicated that its twenty-seven carbons (Table 4) were assigned to four carbonyls, six pairs of double bonds, two oxymethines, one methine, four methylenes and four methyls. These carbon types of **17** were very similar to those of hygrocin B (**15**). Compared to **15**, the NMR spectra of **17** showed additional signals for one non-protonated olefinic carbon and one methylene group at  $\delta_{\text{C}}$  37.7 and  $\delta_{\text{H}}$  2.90 (2H, d,  $J = 7.2$  Hz) (Table 4) and lacked the signals for one carbonyl carbon, one protonated olefinic carbon and the non-protonated carbon at  $\delta_{\text{C}}$  52.6 (C-4) (Table S7), which were observed in the NMR spectra of **15**. Further analyses of the HMQC, COSY and HMBC correlations (Figure 5) of **17** indicated that **17** had a  $\text{C}_3\text{-C}_4$  double bond, but did not have the lactone structure existed in **15**. Therefore, compound **17** was a seco-derivative of **15**. A shared biogenesis suggested that **17** and **15** should have the same 14*S*, 17*S*, 18*S*-configuration. Analyses described above resulted in the identification of **17** as a previously undescribed naphthoquinone ansamycin, named hygrocin T. Its  $^{13}\text{C}$  and  $^1\text{H}$  NMR data (Table 4) were assigned based on the HMQC, COSY and HMBC correlations (Figure 5).

**Table 4.**  $^{13}\text{C}$  NMR (150 MHz) and  $^1\text{H}$  NMR (600 MHz) data of compound **17** (in  $\text{DMSO-}d_6$ ).

No.	$\delta_{\text{C}}$ , Type	$\delta_{\text{H}}$ , Multi. (J in Hz)	No.	$\delta_{\text{C}}$ , Type	$\delta_{\text{H}}$ , Multi. (J in Hz)
1	171.8, C	-	10	180.1, C	-
2	37.7, $\text{CH}_2$	2.90, d (7.2)	10a	138.6, C	-
3	125.5, CH	5.83, td (7.2, 1.2)	11	208.5, C	-
4	136.4, C	-	12	42.5, $\text{CH}_2$	2.76, m; 2.67, m
4a	130.1, C	-	13	29.7, $\text{CH}_2$	1.95, m; 1.67, m
4b	21.4, $\text{CH}_3$	2.13, s	14	45.2, CH	2.00, m
5	185.4, C	-	14a	29.2, $\text{CH}_2$	1.49, m; 1.28, m
5a	131.8, C	-	14b	12.3, $\text{CH}_3$	0.90, t (7.5)
6	124.3, C	-	15	138.6, CH	5.47, dd (15.8, 6.8)
7	158.8, C	-	16	131.3 <sup>a</sup> , CH	5.43, dd (15.8, 6.3)
8	133.0, C	-	17	78.6, CH	3.76, t (6.3)
8a	17.0, $\text{CH}_3$	2.35, s	18	72.0, CH	3.53, m
9	131.3 <sup>a</sup> , CH	7.92, s	18a	19.4, $\text{CH}_3$	1.05, d (6.3)
9a	131.2 <sup>a</sup> , C	-			

<sup>a</sup> Interchangeable chemical shifts.

Compound **18** was obtained as a yellow amorphous powder and its HRESIMS gave an ion peak at  $m/z$   $[\text{M}-\text{H}]^-$  282.0770, corresponding to a molecular formula  $\text{C}_{16}\text{H}_{13}\text{NO}_4$  with eleven degrees of unsaturation. Based on the analyses of its  $^1\text{H}$ ,  $^{13}\text{C}$ , DEPT and HMQC NMR spectra, the sixteen carbons were assigned to three carbonyls ( $\delta_{\text{C}}$  184.2, 177.4, 169.3), five pairs of double bonds, one methylene ( $\delta_{\text{C}}$  36.4) and two methyl groups ( $\delta_{\text{C}}$  20.8, 16.3) (Table 5). The three carbonyl and five pairs of double bonds accounted for eight out of the eleven degrees of unsaturation required by the molecular formula, suggesting that **18** had a structure with three rings. Above evidence, together with further analyses of its COSY and HMBC correlations (Figure 5), demonstrated that the core structure of **18** was similar to that of **17** with the only difference being the absence in **18** of the side chain attached. Therefore, the structure of **18** was elucidated as a previously unreported naphthoquinone ansamycin, named hygrocin U. The  $^{13}\text{C}$  and  $^1\text{H}$  NMR data (Table 5) assignment of **18** was made based on the HMQC, COSY and HMBC correlations (Figure 5).

**Table 5.**  $^{13}\text{C}$  NMR (150 MHz) and  $^1\text{H}$  NMR (600 MHz) data of compounds **18** and **23** (in  $\text{DMSO-}d_6$ ).

No.	18		No.	23	
	$\delta_{\text{C}}$ , Type	$\delta_{\text{H}}$ , Multi. (J in Hz)		$\delta_{\text{C}}$ , Type	$\delta_{\text{H}}$ , Multi. (J in Hz)
1	169.3, C	-	1	135.6, C	-
2	36.4, $\text{CH}_2$	2.83, d (7.1)	2	136.6, C	-
3	123.7, CH	5.79, t (7.1)	3	125.3, CH	7.41, d (7.5)
4	134.2, C	-	4	126.4 <sup>b</sup> , CH	7.13, m
4a	127.8, C	-	5	126.3 <sup>b</sup> , CH	7.12, m
4b	20.8, $\text{CH}_3$	2.09, s	6	130.7, CH	7.15, m
5	184.2, C	-	7	37.5, $\text{CH}_2$	3.08, dd (14.1, 3.6); 2.64, dd (14.1, 9.3)
5a	132.9, C	-	8	71.9, CH	3.92, ddd (9.3, 6.2, 3.6)
6	112.1, CH	7.19, s	9	176.0, C	-
7	165.6 <sup>a</sup> , C	-	10	128.6, CH	6.74, dd (15.8, 1.8)
8	131.1, C	-	11	126.7, CH	6.09, dq (15.8, 6.5)
8a	16.3, $\text{CH}_3$	2.19, s	12	18.7, $\text{CH}_3$	1.86, dd (6.5, 1.8)
9	129.1, CH	7.75, s	OH-8	-	5.42, d (6.2)
9a	119.6 <sup>a</sup> , C	-	NH <sub>2</sub> -9	-	7.25, s; 7.16, s
10	177.4, C	-			
10a	137.6, C	-			
OH-7	-	9.34, 1H, s			

<sup>a</sup> The data were observed from HMBC correlations; <sup>b</sup> The data may be interchanged.

The molecular formula  $C_{12}H_{15}NO_2$  of **23** was determined by its HRESIMS ion peaks at  $m/z$  206.1175  $[M+H]^+$  and 228.0995  $[M+Na]^+$  as well as  $^{13}C$  NMR data. The twelve carbons in **23** were assigned to one carbonyl ( $\delta_C$  176.0), eight olefinic carbons, one oxymethine ( $\delta_C$  71.9), one methylene ( $\delta_C$  37.5) and one methyl group ( $\delta_C$  18.7). COSY correlations (Figure 6) of H-11 ( $\delta_H$  6.09, 1H, m) with H-10 ( $\delta_H$  6.74, 1H, dd, 15.8, 1.8 Hz) and H<sub>3</sub>-12 ( $\delta_H$  1.86, 3H, dd, 6.5, 1.8 Hz) as well as HMBC correlations (Figure 6) of H-12 with C-10 ( $\delta_C$  128.6) and C-11 ( $\delta_C$  126.7) indicated the existence of a 1-propen-1-yl group. Similarly, a “-CH<sub>2</sub>-CH(OH)-CO-” structural fragment was established based on the COSY correlations of H-8 ( $\delta_H$  3.92, 1H, ddd, 9.3, 6.2, 3.6 Hz) with H-7 ( $\delta_H$  3.08, 1H, dd, 14.1, 3.6 Hz; 2.64, 1H, dd, 14.1, 9.3 Hz) and OH-8 ( $\delta_H$  5.42, 1H, d, 6.2 Hz) as well as HMBC correlations of H-7 with C-9 ( $\delta_C$  176.0) and OH-8 with C-7 ( $\delta_C$  37.5), C-8 ( $\delta_C$  71.9) and C-9. In the downfield area ( $\delta_H$  6.09–7.60) of the  $^1H$  NMR spectrum of **23**, there were signals for six olefinic protons. The 1-propen-1-yl group accounted for two olefinic protons and two olefinic carbons and the remaining four olefinic protons and six olefinic carbons were assigned to an aromatic ring. HMBC correlations of H-10 with C-1 ( $\delta_C$  135.6), C-2 ( $\delta_C$  136.6) and C-3 ( $\delta_C$  125.3) and H-3 ( $\delta_H$  7.41, 1H, d, 7.5 Hz) with C-10 established the linkage of the 1-propen-1-yl at C-2. In the same way, the positioning of the “-CH<sub>2</sub>-CH(OH)-CO-” group at C-1 was indicated by HMBC correlations of H-6 ( $\delta_H$  7.15, 1H, m) with C-7, H-7 with C-2 and C-6 ( $\delta_C$  130.7) and H-8 with C-1. In addition, the  $^1H$  NMR spectrum of **23** showed two noncarbonated proton signals at  $\delta_H$  7.25 (1H, s) and 7.16 (1H, s), which were assigned to NH<sub>2</sub>-9. The HRESIMS data also supported a -NH<sub>2</sub> group at C-9, rather than a -OH group. A *trans*-coupling constant value of 15.8 Hz ( $^3J_{H_{10}/H_{11}}$ ) indicated a 10*E*-configuration, while the absolute configuration at C-8 was determined based on the results (Figure 6 and Tables S16–S19) from ECD calculations. The ECD spectrum of **23** displayed positive and negative Cotton effects at 215 and 244 nm, respectively, which closely matched those of the ECD curve calculated for 8*R*-**23**. Based on the foregoing evidence, the structure of **23** was identified as a previously undescribed phenylpropanamide analogue, named streptophenylpropanamide A. Its  $^{13}C$  and  $^1H$  NMR data are reported in Table 5.

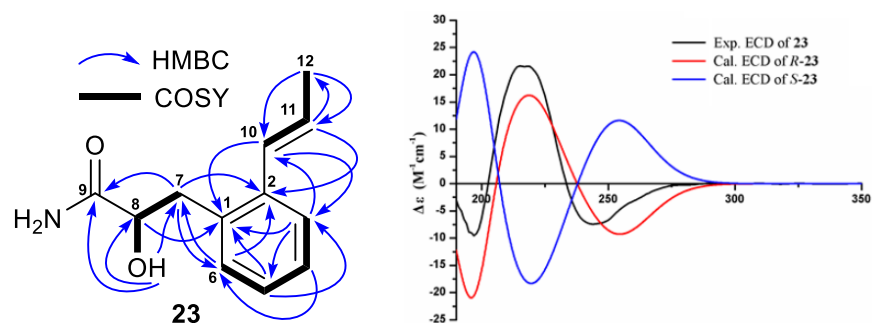


**Figure 6.** COSY and key HMBC correlations of streptobenzenepropanamide A (**23**) and the experimental ECD spectrum of streptobenzenepropanamide A (**23**) and the calculated ECD curves of the model molecules of *R*-**23** and *S*-**23** at the b3lyp/6-311+g (d, p) level.

## 2.2. Biological Activity Evaluation

Sulforhodamine B (SRB) assay was applied to determine the activity of all thirty isolated compounds (**1–30**) against the proliferation of glioma cells. Doxorubicin was used as a positive control. The results (Table 6) indicated that compounds **1**, **2**, **4**, **8**, **11**, **12**, **22** and **30** showed potent antiproliferative activity against both glioma U87MG and U251 cells with IC<sub>50</sub> values ranging from 0.16 to 10.46  $\mu$ M. Compounds **27** and **28** also had activity in inhibiting the proliferation of glioma U87MG and U251 cells with IC<sub>50</sub> values of 11.18 and 19.39  $\mu$ M, respectively. Among all the active compounds, hygrocin C (**1**) showed the strongest activity (IC<sub>50</sub>: 0.16 and 0.35  $\mu$ M), followed by hygrocin D (**2**) (IC<sub>50</sub>: 0.39 and 2.63  $\mu$ M). Compounds **1–18** were eighteen naphthoquinone ansamycins. It was noted that the active ring closed compounds hygrocins C (**1**), D (**2**) and F (**4**) had a 3*Z*-configuration,

compared to the inactive ring closed compounds hygrocin E (3), K (5) and L (6) with a 3E-configuration. However, although both hygrocin M (7) and N (8) had the 3Z-configuration, they exhibited significantly different activities due to the different positioning of the ring closure at the C-6 or C-7 position. In addition, most of the ring open compounds hygrocin O (9), P (10), S (13) and T (17) and degra-hygrocin A (14) were inactive. However, the ring open compounds hygrocin Q (11) and R (12), the methyl esters of hygrocin O (9) and P (10), respectively, were active. These analyses of the structure–activity relationship indicated that a small change in the structure of this class of compounds had significant influence on their antiglioma activities.

**Table 6.** Antiglioma and antibacterial activities of compounds.

Compounds	Glioma Cells (IC <sub>50</sub> : μM)		Microorganisms (MIC: μg/mL)	
	U87MG	U251	MRSA	<i>Escherichia coli</i>
1	0.16 ± 0.01	0.35 ± 0.01	NA	NA
2	0.39 ± 0.04	2.63 ± 0.47	NA	NA
4	0.57 ± 0.09	7.33 ± 0.20	NA	NA
8	8.17 ± 0.17	7.04 ± 0.28	15	8
9	NA	NA	24	20
11	8.81 ± 0.80	10.46 ± 0.27	NA	NA
12	8.32 ± 0.38	7.86 ± 0.26	9	16
17	NA	NA	44	25
18	34.68 ± 0.58	>50	3	6
21	NA	NA	10	16
22	6.18 ± 0.18	8.13 ± 0.56	3	8
26	NA	NA	5	12
27	11.18 ± 0.92	14.64 ± 1.73	6	28
28	19.39 ± 0.67	13.42 ± 1.71	8	48
30	1.64 ± 0.06	1.35 ± 0.05	NA	NA
Doxorubicin	0.43 ± 0.01	4.18 ± 0.39	NT	NT
Vancomycin	NT	NT	0.25	NT
Gentamicin	NT	NT	0.50	0.25

NA: No activity at a concentration of 50 μM or 50 μg/mL; NT: No testing.

The activity of compounds 1–30 in inhibiting the growth of methicillin-resistant *Staphylococcus aureus* (MRSA) and *Escherichia coli* was also evaluated. The results (Table 6) showed that compounds 8, 9, 12, 17, 18, 21, 22 and 26–28 exhibited antibacterial activity against both MRSA and *E. coli* with MIC values of 3–48 μg/mL.

### 3. Experimental Section

#### 3.1. General Procedures

Optical rotation (OR), ultraviolet–visible (UV), electronic circular dichroism (ECD) and infrared (IR) spectra were recorded on an Autopol I polarimeter (Rudolph Research Analytical, Hackettstown, NJ, USA), a METASH UV-8000 spectrometer (Shanghai METASH Instruments Co. Ltd., Shanghai, China), a JASCO J-815 spectropolarimeter (JASCO Co., Tokyo, Japan) and a Nicolet™ IS™ 10 FT-IR spectrometer (Thermo Fisher Scientific, Waltham, MA, USA), respectively. HRESIMS data were acquired on an Agilent 6230 TOF LC/MS spectrometer (Agilent Technologies Co. Ltd., Santa Clara, CA, USA). NMR spectra were obtained on a JEOL 600 spectrometer (JEOL Co. Ltd., Tokyo, Japan) using standard programs and acquisition parameters and chemical shift values were expressed in δ (ppm) relative to DMSO-d<sub>6</sub> (δ<sub>C</sub> 39.5, δ<sub>H</sub> 2.50), MeOH-d<sub>4</sub> (δ<sub>C</sub> 49.15, δ<sub>H</sub> 3.31) or acetone-d<sub>6</sub> (δ<sub>C</sub> 29.8, δ<sub>H</sub> 2.05). Diaion HP-20 (Mitsubishi Chemical, Tokyo, Japan), silica gel (100–200 mesh, Qingdao Marine Chemical Co., Ltd., Qingdao, China), octadecyl-functionalized silica gel (ODS, Cosmosil 75C<sub>18</sub>-Prep, Nacalai Tesque Inc., Kyoto, Japan) and sephadex LH-20 (GE Healthcare, Waukesha, WI, USA) were used for column chromatography. HPLC separation was performed on a CXTH LC-3000 preparative HPLC system (Beijing Chuangxin Tongheng

Science & Technology Co. Ltd., Beijing, China) with column A (CT-30, 280 × 30 mm, 10 μm, Fuji-C<sub>18</sub>) and an Agilent 1260 infinity HPLC system (Agilent Technologies Co. Ltd., Santa Clara, CA, USA) using Zorbax SB-C<sub>18</sub> columns (column B: 250 × 9.4 mm, 5 μm or column C: 250 × 4.6 mm, 5 μm) with a DAD detector. All solvents used for this study were purchased from the Sinopharm Chemical Reagent Co. Ltd. (Shanghai, China). Glioma U87MG (JDS-2568) and U251 (XB-0439) cells used in the experiment were purchased from the Cell Bank of the Chinese Academy of Sciences (Shanghai, China). Methicillin-resistant *Staphylococcus aureus* (MRSA) ATCC 43300 and *Escherichia coli* ATCC 25922 were gifts from Dr. Zhongjun Ma and Dr. Pinmei Wang, respectively. Doxorubicin (DOX) was purchased from Solarbio Science & Technology Co. Ltd. (Beijing, China). Vancomycin and gentamicin were ordered from Meilune Biotechnology Co., Ltd. (Dalian, China). Gauze's agar medium was ordered from the Guangdong Huankai Microbial Science and Technology Co., Ltd. (Guangzhou, China). GYM liquid medium (glucose 4 g, yeast extract 10 g, malt extract 10 g, tap water 1.0 L) was made in the authors' laboratory.

### 3.2. Isolation and Taxonomic Identity of *Streptomyces* sp. ZZ1956

The *Streptomyces* sp. ZZ1956 strain was isolated from a marine mud sample collected from the mangrove area (4.15° S, 119.61° E) of Pangkep District South Sulawesi Province, Indonesia in September 2018. Briefly, the sample (1.0 g) was suspended in sterile water to make dilutions of 10<sup>-2</sup>, 10<sup>-3</sup> and 10<sup>-4</sup> g/mL. Each dilution of 200 μL was spread over the surface of solid Gauze's medium in a Petri dish and then incubated for 10 days at 28 °C. The single ZZ1956 colony from a Petri dish with the 10<sup>-2</sup> g/mL dilution was transferred to a Gauze's agar plate. After growth for another 7 days at 28 °C, the pure strain ZZ1956 colony (Figure S2) was transferred onto Gauze's agar slants and stored at 4 °C for later use. The 16S rDNA sequence analysis of the strain ZZ1956 was conducted by Legenomix (Hangzhou, China). The 16S rDNA sequence of the strain ZZ1956 was deposited in GenBank with an accession number of MT672495. The voucher strain of *Streptomyces* sp. ZZ1956 was preserved at the Laboratory of the Institute of Marine Biology and Pharmacology, Ocean College, Zhoushan campus, Zhejiang University, Zhoushan, China.

### 3.3. Mass Culture of the Strain ZZ1956

Colonies of the strain ZZ1956 from the Gauze's agar plate were inoculated into 500 mL Erlenmeyer flasks, each containing 250 mL of sterile GYM liquid medium and then incubated at 28 °C for 3 days on a rotary shaker (180 rpm) to prepare the seed broth. The seed broth (10 mL) was then transferred into a 500 mL Erlenmeyer flask containing 250 mL sterilized GYM liquid medium. A total of 60 L (240 bottles) of culture was prepared for this study and incubated at 28 °C for 15 days under shaking (180 rpm) condition.

### 3.4. Extraction and Isolation of Compounds 1–30

The 60-L culture of strain ZZ1956 was centrifuged to yield supernatant and mycelia. The mycelia were extracted with MeOH three times (3 L, each time) to give a MeOH extract solution. The supernatant was applied to a Dianion HP-20 column eluted with water and then MeOH to obtain a MeOH elution. The MeOH extract solution and MeOH elution were combined and dried in vacuo to give a crude extract, which was further partitioned with EtOAc three times to give an EtOAc extract (24 g). The EtOAc extract was subjected to a column of silica gel eluted with mixtures of cyclohexane/EtOAc (10/1, 8/1, 5/1, 2/1, 1/1, v/v), EtOAc, and MeOH to give ten fractions (Frs. A–J) based on the results of TLC and HPLC analyses.

Fr. A was purified by HPLC using column C (mobile phase: MeCN/H<sub>2</sub>O, 65/35; flow rate: 0.8 mL/min; UV detection: 210 nm) to give **26** (4.8 mg, t<sub>R</sub> 15.4 min). Fractions B and D were separated on HPLC column B (flow rate: 1 mL/min; UV detection: 210 nm) to give **24** (3.0 mg, t<sub>R</sub> 25.0 min, MeOH/H<sub>2</sub>O, 40/60) and **22** (4.4 mg, t<sub>R</sub> 24.4 min, MeOH/H<sub>2</sub>O, 67/37), respectively.

Fr. C was subjected to a sephadex LH-20 column eluted with 70% MeOH to yield three subfractions (Frs. C<sub>1</sub>–C<sub>3</sub>). Fr. C<sub>1</sub> was further separated on column C (mobile phase: MeOH/H<sub>2</sub>O, 34/66; flow rate: 0.8 mL/min; UV detection: 210 nm) to give **19** (1.2 mg, t<sub>R</sub> 15.7 min) and **20** (3.8 mg, t<sub>R</sub> 18.6 min). Compound **18** (1.7 mg, t<sub>R</sub> 25.5 min) was obtained from Fr. C<sub>2</sub> through HPLC purification using column B (mobile phase: MeOH/H<sub>2</sub>O, 67/33; flow rate: 1 mL/min; UV detection: 280 nm).

Each of Fr. E, Fr. F and Fr. H was separated by preparative HPLC using column A (flow rate: 10 mL/min; UV detection: 210 nm). Compounds **21** (4.9 mg, t<sub>R</sub> 19.5 min), **15** (21.0 mg, t<sub>R</sub> 24.3 min) and **16** (7.4 mg, t<sub>R</sub> 44.1 min) were obtained from Fr. E using a mobile phase (MeOH/0.1% HOAc in H<sub>2</sub>O, 70/30), **14** (8.0 mg, t<sub>R</sub> 26.2 min, MeOH/0.1% HOAc in H<sub>2</sub>O, 65/35) was purified from Fr. H and five subfractions (Frs. F<sub>1</sub>–F<sub>5</sub>) were obtained from Fr. F using a gradient mobile phase (MeOH/0.1% HOAc in H<sub>2</sub>O, 30/70–100/0) in 40 min. Each of Frs. F<sub>1</sub>–F<sub>5</sub> was purified by HPLC column B (flow rate: 1 mL/min; UV detection: 210 nm) to give **1** (28.0 mg, t<sub>R</sub> 23.1 min, MeCN/H<sub>2</sub>O, 33/67), **7** (3.3 mg, t<sub>R</sub> 23.7 min, MeOH/H<sub>2</sub>O, 55/45), **3** (6.0 mg, t<sub>R</sub> 57.5 min, MeCN/H<sub>2</sub>O, 30/70), **2** (19.0 mg, t<sub>R</sub> 26.3 min, MeCN/H<sub>2</sub>O, 45/55) and **8** (3.3 mg, t<sub>R</sub> 33.3 min, MeOH/H<sub>2</sub>O, 66/34).

Fr. G was fractionated by an ODS column eluted with 65%, 75% and 100% MeOH to give three subfractions (Frs. G<sub>1</sub>–G<sub>3</sub>) based on the results of TLC and HPLC analyses. Compound **29** (4.4 mg, t<sub>R</sub> 28.2 min) was obtained from Fr. G<sub>2</sub> through HPLC purification using column B (mobile phase: MeCN/0.1% HOAc in H<sub>2</sub>O, 30/70; flow rate: 1 mL/min; UV detection: 256 nm). Fr. G<sub>3</sub> was further separated by HPLC column A (mobile phase: MeOH/0.1% HOAc in H<sub>2</sub>O, 70/30; flow rate: 10 mL/min; UV detection: 210 nm) to give six subfractions (Frs. G<sub>3a</sub>–G<sub>3f</sub>). Fr. G<sub>3a</sub> continued to be separated on the same column A with the same flow rate and UV detection to give Fr. G<sub>3aa</sub> and Fr. G<sub>3ab</sub> (MeOH/0.1% HOAc in H<sub>2</sub>O, 55/45). Further purification by HPLC column B (flow rate: 1 mL/min; UV detection: 256 nm) yielded compounds **5** (5.9 mg, t<sub>R</sub> 48.8 min, MeCN/H<sub>2</sub>O, 27/73) from Fr. G<sub>3aa</sub>, **6** (2.3 mg, t<sub>R</sub> 43.7 min, MeCN/H<sub>2</sub>O, 33/67) from Fr. G<sub>3ab</sub>, **23** (2.0 mg, t<sub>R</sub> 21.9 min, MeOH/0.1% HOAc in H<sub>2</sub>O, 65/35) from Fr. G<sub>3b</sub>, **4** (16.0 mg, t<sub>R</sub> 24.1 min, MeCN/H<sub>2</sub>O, 45/55) from Fr. G<sub>3c</sub>, **13** (3.0 mg, t<sub>R</sub> 32.3 min) and **17** (8.0 mg, t<sub>R</sub> 37.1 min, MeCN/0.1% HOAc in H<sub>2</sub>O, 39/61) from Fr. G<sub>3d</sub>, **9** (2.8 mg, t<sub>R</sub> 30.0 min), **10** (2.8 mg, t<sub>R</sub> 38.5 min), **12** (2.5 mg, t<sub>R</sub> 64.2 min) and **11** (2.2 mg, t<sub>R</sub> 77.1 min, MeOH/0.1% HOAc in H<sub>2</sub>O, 70/30) from Fr. G<sub>3f</sub>.

Similarly, Fr. I was also applied to an ODS column eluted with 50%, 70% and 100% MeOH to yield three subfractions (Frs. I<sub>1</sub>–I<sub>3</sub>). Fr. I<sub>1</sub> was further separated on HPLC column A (flow rate: 10 mL/min; UV detection: 210 nm) with a gradient mobile phase from 40% to 100% MeOH in 40 min to give **25** (2.0 mg, t<sub>R</sub> 15.8 min); while compound **30** (20.0 mg, t<sub>R</sub> 32.4 min) was obtained from Fr. I<sub>3</sub> by separating on column B (mobile phase: MeOH/H<sub>2</sub>O, 95/5; flow rate: 1 mL/min; UV detection: 256 nm).

Finally, Fr. J was fractionated on an ODS column eluted with 30%, 40%, 60%, 70% and 100% MeOH to give Fr. J<sub>1</sub> and Fr. J<sub>2</sub> based on the results of HPLC analyses. Fr. J<sub>1</sub> was further separated on column A (flow rate: 10 mL/min; UV detection: 210 nm) with a gradient mobile phase from 40% to 100% MeOH in 40 min to give Fr. J<sub>1a</sub> and Fr. J<sub>1b</sub>. Compounds **27** (9.0 mg, t<sub>R</sub> 24.3 min) and **28** (2.0 mg, t<sub>R</sub> 42.3 min) were obtained from Fr. J<sub>1a</sub> through HPLC purification using column B (mobile phase: MeCN/H<sub>2</sub>O, 33/67; flow rate: 1 mL/min; UV detection: 210 nm).

### 3.5. Compound Characterization Data

Hygrocin K (**5**): Light yellow oil; molecular formula C<sub>28</sub>H<sub>31</sub>NO<sub>8</sub>; [α]<sub>D</sub><sup>20</sup> −65.5 (c 0.10, MeOH); UV (MeOH) λ<sub>max</sub> (log ε) 203 (4.39), 271 (4.04), 304 (4.00) nm; IR (ATR) ν<sub>max</sub> 3320, 2962, 2929, 2870, 1662, 1627, 1569, 1322, 1237, 1190, 1131, 1051, 976, 857, 733 cm<sup>−1</sup>; <sup>13</sup>C NMR data (150 MHz), Table 1, <sup>1</sup>H NMR data (600 MHz), Table 2; HRESIMS *m/z* 508.1969 [M−H]<sup>−</sup> (calcd for C<sub>28</sub>H<sub>30</sub>NO<sub>8</sub><sup>−</sup>, 508.1971).

Hygrocin L (**6**): Light yellow oil; molecular formula C<sub>28</sub>H<sub>31</sub>NO<sub>8</sub>; [α]<sub>D</sub><sup>20</sup> +166.6 (c 0.10, MeOH); UV (MeOH) λ<sub>max</sub> (log ε) 203 (4.21), 270 (4.04), 304 (4.03) nm; IR (ATR) ν<sub>max</sub> 3314,

2963, 2928, 2874, 1698, 1657, 1627, 1567, 1239, 1188, 1108, 1029, 976, 857, 810, 735  $\text{cm}^{-1}$ ;  $^{13}\text{C}$  NMR data (150 MHz), Table 1,  $^1\text{H}$  NMR data (600 MHz), Table 2; HRESIMS  $m/z$  508.1979  $[\text{M}-\text{H}]^-$  (calcd for  $\text{C}_{28}\text{H}_{30}\text{NO}_8^-$ , 508.1971).

Hygrocin M (7): Light yellow amorphous powder; molecular formula  $\text{C}_{28}\text{H}_{29}\text{NO}_7$ ;  $[\alpha]_{\text{D}}^{20} +166.7$  (c 0.10, MeOH); UV (MeOH)  $\lambda_{\text{max}}$  (log  $\epsilon$ ) 201 (4.52), 333 (4.11) nm; IR (ATR)  $\nu_{\text{max}}$  3362, 2960, 2930, 2868, 1714, 1655, 1626, 1559, 1446, 1346, 1285, 1134, 1044, 860  $\text{cm}^{-1}$ ;  $^{13}\text{C}$  NMR data (150 MHz), Table 1,  $^1\text{H}$  NMR data (600 MHz), Table 2; HRESIMS  $m/z$  490.1875  $[\text{M}-\text{H}]^-$  (calcd for  $\text{C}_{28}\text{H}_{28}\text{NO}_7^-$ , 490.1866).

Hygrocin N (8): Light yellow amorphous powder; molecular formula  $\text{C}_{28}\text{H}_{29}\text{NO}_7$ ;  $[\alpha]_{\text{D}}^{20} +270.0$  (c 0.10, MeOH); UV (MeOH)  $\lambda_{\text{max}}$  (log  $\epsilon$ ) 201 (4.55), 336 (4.26) nm; IR (ATR)  $\nu_{\text{max}}$  3275, 2963, 2927, 2877, 1709, 1650, 1617, 1567, 1466, 1338, 1282, 1249, 1132, 1079, 859, 736  $\text{cm}^{-1}$ ;  $^{13}\text{C}$  NMR data (150 MHz), Table 1,  $^1\text{H}$  NMR data (600 MHz), Table 2; HRESIMS  $m/z$  492.2010  $[\text{M}+\text{H}]^+$  (calcd for  $\text{C}_{28}\text{H}_{30}\text{NO}_7$ , 492.2022), 514.1832  $[\text{M}+\text{Na}]^+$  (calcd for  $\text{C}_{28}\text{H}_{29}\text{NNaO}_7$ , 514.1842) and 490.1871  $[\text{M}-\text{H}]^-$  (calcd for  $\text{C}_{28}\text{H}_{28}\text{NO}_7^-$ , 490.1866).

Hygrocin O (9): Red amorphous powder; molecular formula  $\text{C}_{28}\text{H}_{31}\text{NO}_8$ ;  $[\alpha]_{\text{D}}^{20} -21.5$  (c 0.10, MeOH); UV (MeOH)  $\lambda_{\text{max}}$  (log  $\epsilon$ ) 201 (4.65), 334 (4.33) nm; IR (ATR)  $\nu_{\text{max}}$  3257, 2959, 2926, 2872, 1697, 1652, 1600, 1580, 1343, 1257, 1204, 1135, 1022, 978  $\text{cm}^{-1}$ ;  $^{13}\text{C}$  NMR data (150 MHz), Table 1,  $^1\text{H}$  NMR data (600 MHz), Table 3; HRESIMS  $m/z$  508.1975  $[\text{M}-\text{H}]^-$  (calcd for  $\text{C}_{28}\text{H}_{30}\text{NO}_8^-$ , 508.1971).

Hygrocin P (10): Red amorphous powder; molecular formula  $\text{C}_{28}\text{H}_{31}\text{NO}_8$ ;  $[\alpha]_{\text{D}}^{20} -55.5$  (c 0.10, MeOH); UV (MeOH)  $\lambda_{\text{max}}$  (log  $\epsilon$ ) 201 (4.29), 334 (4.07) nm; IR (ATR)  $\nu_{\text{max}}$  3229, 2966, 2926, 2875, 1705, 1651, 1622, 1576, 1467, 1339, 1263, 1245, 1120, 1063, 1018, 976, 855, 737  $\text{cm}^{-1}$ ;  $^{13}\text{C}$  NMR data (150 MHz), Table 1,  $^1\text{H}$  NMR data (600 MHz), Table 3; HRESIMS  $m/z$  508.1974  $[\text{M}-\text{H}]^-$  (calcd for  $\text{C}_{28}\text{H}_{30}\text{NO}_8^-$ , 508.1971).

Hygrocin Q (11): Red amorphous powder; molecular formula  $\text{C}_{29}\text{H}_{33}\text{NO}_8$ ;  $[\alpha]_{\text{D}}^{20} -16.0$  (c 0.10, MeOH); UV (MeOH)  $\lambda_{\text{max}}$  (log  $\epsilon$ ) 201 (4.22), 335 (4.10) nm; IR (ATR)  $\nu_{\text{max}}$  3345, 2960, 2925, 2875, 1714, 1655, 1629, 1598, 1573, 1435, 1349, 1263, 1188, 1149, 1020, 978, 851, 755  $\text{cm}^{-1}$ ;  $^{13}\text{C}$  NMR data (150 MHz), Table 1,  $^1\text{H}$  NMR data (600 MHz), Table 3; HRESIMS  $m/z$  522.2125  $[\text{M}-\text{H}]^-$  (calcd for  $\text{C}_{29}\text{H}_{32}\text{NO}_8^-$ , 522.2128).

Hygrocin R (12): Red amorphous powder; molecular formula  $\text{C}_{29}\text{H}_{33}\text{NO}_8$ ;  $[\alpha]_{\text{D}}^{20} -40.0$  (c 0.10, MeOH); UV (MeOH)  $\lambda_{\text{max}}$  (log  $\epsilon$ ) 201 (4.14), 335 (4.09) nm; IR (ATR)  $\nu_{\text{max}}$  3376, 2959, 2927, 2872, 1696, 1653, 1596, 1578, 1441, 1339, 1261, 1202, 1136, 1064, 976, 851, 802, 728  $\text{cm}^{-1}$ ;  $^{13}\text{C}$  NMR data (150 MHz), Table 1,  $^1\text{H}$  NMR data (600 MHz), Table 3; HRESIMS  $m/z$  522.2132  $[\text{M}-\text{H}]^-$  (calcd for  $\text{C}_{29}\text{H}_{32}\text{NO}_8^-$ , 522.2128).

Hygrocin S (13): Red amorphous powder; molecular formula  $\text{C}_{28}\text{H}_{31}\text{NO}_8$ ;  $[\alpha]_{\text{D}}^{20} -21.6$  (c 0.10, MeOH); UV (MeOH)  $\lambda_{\text{max}}$  (log  $\epsilon$ ) 201 (4.13), 333 (4.06) nm; IR (ATR)  $\nu_{\text{max}}$  3240, 2962, 2870, 1709, 1655, 1574, 1350, 1222, 1130, 1068, 976, 855  $\text{cm}^{-1}$ ;  $^{13}\text{C}$  NMR data (150 MHz), Table 1,  $^1\text{H}$  NMR data (600 MHz), Table 3; HRESIMS  $m/z$  508.1975  $[\text{M}-\text{H}]^-$  (calcd for  $\text{C}_{28}\text{H}_{30}\text{NO}_8^-$ , 508.1971).

Hygrocin T (17): Yellow amorphous powder; molecular formula  $\text{C}_{27}\text{H}_{31}\text{NO}_7$ ;  $[\alpha]_{\text{D}}^{20} -34.0$  (c 0.10, MeOH); UV (MeOH)  $\lambda_{\text{max}}$  (log  $\epsilon$ ) 204 (4.35), 211 (4.35), 279 (4.36), 308 (4.10) nm; IR (ATR)  $\nu_{\text{max}}$  3324, 2961, 2925, 2874, 1694, 1655, 1567, 1457, 1339, 1261, 1188, 1151, 1012, 973, 806, 735  $\text{cm}^{-1}$ ;  $^{13}\text{C}$  NMR (150 MHz) and  $^1\text{H}$  NMR (600 MHz) data, Table 4; HRESIMS  $m/z$  480.2024  $[\text{M}-\text{H}]^-$  (calcd for  $\text{C}_{27}\text{H}_{30}\text{NO}_7^-$ , 480.2022).

Hygrocin U (18): Light yellow amorphous powder; molecular formula  $\text{C}_{16}\text{H}_{13}\text{NO}_4$ ; UV (MeOH)  $\lambda_{\text{max}}$  (log  $\epsilon$ ) 201 (4.21), 211 (4.12), 280 (4.17), 307 (3.81) nm; IR (ATR)  $\nu_{\text{max}}$  3319, 2956, 2920, 2849, 1674, 1651, 1567, 1466, 1327, 1265, 1206, 1146  $\text{cm}^{-1}$ ;  $^{13}\text{C}$  NMR (150 MHz) and  $^1\text{H}$  NMR (600 MHz) data, Table 5; HRESIMS  $m/z$  282.0770  $[\text{M}-\text{H}]^-$  (calcd for  $\text{C}_{16}\text{H}_{12}\text{NO}_4^-$ , 282.0766).

Streptobenzenepropanamide A (23): White amorphous powder; molecular formula  $\text{C}_{12}\text{H}_{15}\text{NO}_2$ ;  $[\alpha]_{\text{D}}^{20} +12.4$  (c 0.10, MeOH); ECD (15 mg/L, MeOH)  $\lambda_{\text{max}}$  ( $\Delta\epsilon$ ) 215 (+20.14), 244 (-6.93) nm; UV (MeOH)  $\lambda_{\text{max}}$  (log  $\epsilon$ ) 202 (4.16), 248 (3.91) nm; IR (ATR)  $\nu_{\text{max}}$  3333, 2963, 2925, 2852, 1665, 1578, 1447, 1406, 1380, 1261, 1094, 1074, 965, 802, 751  $\text{cm}^{-1}$ ;  $^{13}\text{C}$  NMR (150

MHz) and  $^1\text{H}$  NMR (600 MHz) data, Table 5; HRESIMS  $m/z$  206.1175  $[\text{M}+\text{H}]^+$  (calcd for  $\text{C}_{12}\text{H}_{16}\text{NO}_2^+$ , 206.1181) and 228.0995  $[\text{M}+\text{Na}]^+$  (calcd for  $\text{C}_{12}\text{H}_{15}\text{NNaO}_2^+$ , 228.1000).

### 3.6. MTPA Esterification Hygrocin N (8)

Hygrocin N (**8**, 3 mg) was dissolved in 2 mL anhydrous pyridine. Half of the sample solution was added either (R)- or (S)- $\alpha$ -methoxy- $\alpha$ -(trifluoromethyl)-phenylacetyl chloride (MTPA-Cl, 45  $\mu\text{L}$ ). The mixture was stirred at room temperature for 24 h and then added MeOH (0.5 mL) to stop the reaction. The reaction products were separated by HPLC using column B with a flow rate of 1 mL/min and UV detection of 210 nm to furnish (S)-MTPA ester **8s** (1.0 mg,  $t_{\text{R}}$  22.5 min, MeOH/H<sub>2</sub>O, 92/8) or (R)-MTPA ester **8r** (1.2 mg,  $t_{\text{R}}$  22.5 min, MeOH/H<sub>2</sub>O, 92/8).

(S)-MTPA ester **8s**:  $^1\text{H}$  NMR data (600 MHz, in MeOH- $d_4$ ), Table S15; HRESIMS  $m/z$  924.2815  $[\text{M}+\text{H}]^+$  (calcd for  $\text{C}_{48}\text{H}_{44}\text{F}_6\text{NO}_{11}^+$ , 924.2819) and 946.2640  $[\text{M}+\text{Na}]^+$  (calcd for  $\text{C}_{48}\text{H}_{43}\text{F}_6\text{NNaO}_{11}^+$ , 946.2638).

(R)-MTPA ester **8r**:  $^1\text{H}$  NMR data (600 MHz, in MeOH- $d_4$ ), Table S15; HRESIMS  $m/z$  924.2824  $[\text{M}+\text{H}]^+$  (calcd for  $\text{C}_{48}\text{H}_{44}\text{F}_6\text{NO}_{11}^+$ , 924.2819) and 946.2628  $[\text{M}+\text{Na}]^+$  (calcd for  $\text{C}_{48}\text{H}_{43}\text{F}_6\text{NNaO}_{11}^+$ , 946.2638).

### 3.7. ECD Calculations

The details of ECD calculations for compound **23** were described as our previous publications [19,20].

### 3.8. Sulforhodamine B (SRB) Assay

The culture of human glioma cells and the SRB assay were according to our previous reports [19,33].

### 3.9. Antibacterial Activity Determination

The antibacterial activity of the tested compounds against MRSA and *E. coli* was evaluated by the micro broth dilution method [34] using vancomycin and gentamicin as positive controls and DMSO as a negative control.

## 4. Conclusions

Marine-derived actinomycetes from the genus *Streptomyces* continue to be one of the main resources for the discovery of novel bioactive natural products. A chemical investigation of the extract prepared from a scaled-up culture of the marine-derived actinomycete *Streptomyces* sp. ZZ1956 in GYM liquid medium resulted in the isolation and identification of thirty compounds (**1–30**), including twelve previously undescribed compounds, namely, hygrocins K–U (**5–13**, **17**, **18**) and streptophenylpropanamide A (**23**). Compounds **1–18** were naphthalenic ansamycin derivatives and a small change in their structures significantly influenced their antiglioma activity. Hygrocins C (**1**), D (**2**) and F (**4**) structurally characterized with ring closing and 3Z-configuration exhibited potent antiproliferative activity against both human glioma U87MG and U251 cells. Hygrocins N (**8**), O (**9**), R (**12**), T (**17**) and U (**18**), 2-amino-6-hydroxy-7-methyl-1,4-naphthoquinone (**21**), 2-acetamide-6-hydroxy-7-methyl-1,4-naphthoquinone (**22**), 3'-methoxy(1,1',4',1''-terphenyl)-2',6'-diol (**26**), echoside C (**27**) and echoside A (**28**) exhibited antibacterial activity against MRSA and *E. coli*. The data from this study greatly enrich the chemical and bioactive diversities of the ansamycin antibiotics.

**Supplementary Materials:** The following supporting information can be downloaded at: <https://www.mdpi.com/article/10.3390/antibiotics11111455/s1>, Table S1: Sequences producing significant alignments; Table S2: Crystallographic data and structure refinement parameters of hygrocin C (**1**); Tables S3–S14:  $^{13}\text{C}$  and  $^1\text{H}$  NMR data of the known compounds; Table S15:  $^1\text{H}$  NMR data of compound **8s** and **8r**; Tables S16–S19: Data of the ECD calculations of streptobenzenepropanamide A (**23**); Figure S1: 16S rDNA sequence of *Streptomyces* sp. ZZ1956; Figure S2: Colony of strain ZZ1956 cultured in GYM medium; Figures S3–S19: NMR, HRESIMS, UV and IR spectra of hygrocin K (**5**);

Figures S20–S36: NMR, HRESIMS, UV and IR spectra of hygrocin L (6); Figures S37–S52: NMR, HRESIMS, UV and IR spectra of hygrocin M (7); Figures S53–S68: NMR, HRESIMS, UV and IR spectra of hygrocin N (8); Figures S69–S72: <sup>1</sup>H NMR and HRESIMS spectra of 8s and 8r; Figures S73–S88: NMR, HRESIMS, UV and IR spectra of hygrocin O (9); Figures S89–S104: NMR, HRESIMS, UV and IR spectra of hygrocin P (10); Figures S105–S118: NMR, HRESIMS, UV and IR spectra of hygrocin Q (11); Figures S119–S132: NMR, HRESIMS, UV and IR spectra of hygrocin R (12); Figures S133–S146: NMR, HRESIMS, UV and IR spectra of hygrocin S (13); Figures S147–S160: NMR, HRESIMS, UV and IR spectra of hygrocin T (17); Figures S161–S169: NMR, HRESIMS, UV and IR spectra of hygrocin U (18); Figures S170–S182: NMR, HRESIMS, UV and IR spectra of streptobenzenepropanamide A (23).

**Author Contributions:** X.-Y.L. and Z.Z. conceived and designed the experiments; W.Y., A.W.N., K.Y. and M.M. performed the experiments; X.-Y.L. and Z.Z. analyzed the data and wrote the paper. All authors have read and agreed to the published version of the manuscript.

**Funding:** This study was financially supported by the National Natural Science Foundation of China (No. 81773587) and the HPC Center of Zhejiang University (Zhoushan Campus).

**Institutional Review Board Statement:** Not applicable.

**Informed Consent Statement:** Not applicable.

**Data Availability Statement:** All the data in this research are presented in manuscript and supplementary material.

**Acknowledgments:** We thank Chelsea Zhang in New York (NY, USA) for English editing.

**Conflicts of Interest:** The authors declare no conflict of interest.

## References

1. Kang, Q.J.; Shen, Y.M.; Bai, L.Q. Biosynthesis of 3,5-AHBA-derived natural products. *Nat. Prod. Rep.* **2012**, *29*, 243–263. [[CrossRef](#)]
2. Skrzypczak, N.; Przybylski, P. Structural diversity and biological relevance of benzenoid and atypical ansamycins and their congeners. *Nat. Prod. Rep.* **2022**, *39*, 1678–1704. [[CrossRef](#)]
3. Funayama, S.; Cordell, G.A. Ansamycin antibiotics, discovery, classification, biosynthesis and biological activities. *Stud. Nat. Prod. Chem.* **2000**, *23*, 51–106.
4. Eckelmann, D.; Kusari, S.; Spiteller, M. Occurrence and spatial distribution of maytansinoids in *Putterlickia pyracantha*, an unexplored resource of anticancer compounds. *Fitoterapia* **2016**, *113*, 175–181. [[CrossRef](#)] [[PubMed](#)]
5. Kusari, S.; Lamshöft, M.; Kusari, P.; Gottfried, S.; Zühlke, S.; Louven, K.; Hentschel, U.; Kayser, O.; Spiteller, M. Endophytes are hidden producers of maytansine in *Putterlickia* roots. *J. Nat. Prod.* **2014**, *77*, 2577–2584. [[CrossRef](#)] [[PubMed](#)]
6. Wei, F.F.; Wang, Z.S.; Lu, C.H.; Li, Y.Y.; Zhu, J.; Wang, H.X.; Shen, Y.M. Targeted discovery of pentaketide ansamycin aminoansamycins A–G. *Org. Lett.* **2019**, *21*, 7818–7822. [[CrossRef](#)] [[PubMed](#)]
7. Zhang, C.Y.; Zhang, H.R.; Ju, J.H. On-PKS Baeyer-Villiger-type O-atom insertion catalyzed by luciferase-like monooxygenase ovmO during olimycin biosynthesis. *Org. Lett.* **2020**, *22*, 1780–1784. [[CrossRef](#)] [[PubMed](#)]
8. Liu, S.H.; Wei, Y.Y.; Xing, Y.N.; Chen, Y.; Wang, W.; Wang, K.B.; Liang, Y.; Jiao, R.H.; Zhang, B.; Ge, H.M. A BBE-like oxidase, asmF, dictates the formation of naphthalenic hydroxyl groups in ansaseomycin biosynthesis. *Org. Lett.* **2021**, *23*, 3724–3728. [[CrossRef](#)] [[PubMed](#)]
9. Nong, X.H.; Tu, Z.C.; Qi, S.H. Ansamycin derivatives from the marine-derived *Streptomyces* sp. SCSGAA 0027 and their cytotoxic and antiviral activities. *Bioorganic Med. Chem. Lett.* **2020**, *30*, 7168. [[CrossRef](#)] [[PubMed](#)]
10. Ye, X.W.; Anjum, K.; Song, T.F.; Wang, W.L.; Liang, Y.; Chen, M.X.; Huang, H.C.; Lian, X.Y.; Zhang, Z.Z. Antiproliferative cyclodepsipeptides from the marine actinomycete *Streptomyces* sp. P11-23B downregulating the tumor metabolic enzymes of glycolysis, glutaminolysis, and lipogenesis. *Phytochemistry* **2017**, *135*, 151–159. [[CrossRef](#)] [[PubMed](#)]
11. Chen, L.; Chai, W.Y.; Wang, W.L.; Song, T.F.; Lian, X.Y.; Zhang, Z.Z. Cytotoxic bagremycins from mangrove-derived *Streptomyces* sp. Q22. *J. Nat. Prod.* **2017**, *80*, 1450–1456. [[CrossRef](#)] [[PubMed](#)]
12. Chen, M.X.; Chai, W.Y.; Song, T.F.; Ma, M.Z.; Lian, X.Y.; Zhang, Z.Z. Anti-glioma natural products downregulating tumor glycolytic enzymes from marine actinomycetes *Streptomyces* sp. ZZ406. *Sci. Rep.* **2018**, *8*, 72. [[CrossRef](#)] [[PubMed](#)]
13. Song, T.F.; Chen, M.X.; Chai, W.Y.; Zhang, Z.Z.; Lian, X.Y. New bioactive pyrrospirones C-I from a marine-derived fungus *Penicillium* sp. ZZ380. *Tetrahedron* **2018**, *74*, 884–891. [[CrossRef](#)]
14. Song, T.F.; Chen, M.X.; Ge, Z.W.; Chai, W.Y.; Li, X.C.; Zhang, Z.Z.; Lian, X.Y. Bioactive penicypyrrodiether A, an adduct of GKK1032 analogue and phenol A derivative, from a marine-sourced fungus *Penicillium* sp. ZZ380. *J. Org. Chem.* **2018**, *83*, 13395–13401. [[CrossRef](#)] [[PubMed](#)]
15. Song, T.F.; Tang, M.M.; Ge, H.J.; Chen, M.X.; Lian, X.Y.; Zhang, Z.Z. Novel bioactive penicypyrroether A and pyrrospirones J from the marine-derived *Penicillium* sp. ZZ380. *Mar. Drugs* **2019**, *17*, 292. [[CrossRef](#)] [[PubMed](#)]

16. Zhang, D.; Yi, W.W.; Ge, H.J.; Zhang, Z.Z.; Wu, B. Bioactive streptoglutaramides A–J from the marine-derived *Streptomyces* sp. ZZ741. *J. Nat. Prod.* **2019**, *82*, 2800–2808. [[CrossRef](#)] [[PubMed](#)]
17. Qin, L.; Yi, W.W.; Lian, X.Y.; Zhang, Z.Z. Bioactive alkaloids from the actinomycete *Actinoalloteichus* sp. ZZ1866. *J. Nat. Prod.* **2020**, *83*, 2686–2695. [[CrossRef](#)] [[PubMed](#)]
18. Ge, H.J.; Zhang, D.; Shi, M.R.; Lian, X.Y.; Zhang, Z.Z. Antiproliferative activity and potential mechanism of marine-sourced streptoglutaramide H against lung cancer cells. *Mar. Drugs* **2021**, *19*, 79. [[CrossRef](#)] [[PubMed](#)]
19. Yong, K.; Kaleem, S.; Wu, B.; Zhang, Z.Z. New antiproliferative compounds against glioma cells from the marine-sourced fungus *Penicillium* sp. ZZ1750. *Mar. Drugs* **2021**, *19*, 483. [[CrossRef](#)]
20. Yi, W.W.; Lian, X.Y.; Zhang, Z.Z. Cytotoxic metabolites from the marine-associated *Streptomyces* sp. ZZ1944. *Phytochemistry* **2022**, *201*, 113292. [[CrossRef](#)] [[PubMed](#)]
21. Lu, C.H.; Li, Y.Y.; Deng, J.J.; Li, S.R.; Shen, Y.; Wang, H.X.; Shen, Y.M. Hygrocins C–G, cytotoxic naphthoquinone ansamycins from gdmAI-disrupted *Streptomyces* sp. LZ35. *J. Nat. Prod.* **2013**, *76*, 2175–2179. [[CrossRef](#)] [[PubMed](#)]
22. Cai, P.; Kong, F.M.; Ruppen, M.E.; Glasier, G.; Carter, G.T. Hygrocins A and B, naphthoquinone macrolides from *Streptomyces hygroscopicus*. *J. Nat. Prod.* **2005**, *68*, 1736–1742. [[CrossRef](#)] [[PubMed](#)]
23. Sánchez-Ferrando, F. Assignment of quaternary carbons via two-bond heteronuclear selective NOE difference, a useful structure elucidation aid. *Magn. Reson. Chem.* **1985**, *23*, 185–191. [[CrossRef](#)]
24. Nagao, T.; Otsuka, H.; Kohda, H.; Sato, T.; Yamasaki, K. Benzoxazinones from *Coix lachryma-jobi* var. *ma-yuen*. *Phytochemistry* **1985**, *24*, 2959–2962. [[CrossRef](#)]
25. Supong, K.; Sripreechajak, P.; Tanasupawat, S.; Danwisetkanjana, K.; Rachtawee, P.; Pittayakhajonwut, P. Investigation on antimicrobial agents of the terrestrial *Streptomyces* sp. BCC71188. *Appl. Microbiol. Biotechnol.* **2017**, *101*, 533–543. [[CrossRef](#)]
26. Hager, A.; Kuttruff, C.A.; Herrero-Gómez, E.; Trauner, D. Toward the total synthesis of ansalactam A. *Tetrahedron Lett.* **2014**, *55*, 59–62. [[CrossRef](#)]
27. Spiessens, L.I.; Anteunis, M.J.O. NMR studies on imidines. III.  $^1\text{H}$  and  $^{13}\text{C}$  nuclear magnetic resonance study on the tautomerism and geometrical isomerism of 3-iminoisoindolinone and some alkylated derivatives. Observation of E and Z isomers about a free imino grouping. *Bull. Des Sociétés Chim. Belg.* **1983**, *92*, 965–993. [[CrossRef](#)]
28. Chang, S.-S.; Chen, M.-H.; Wang, R.-Z.; Wu, Y.-X.; Yang, G.-H.; Dong, B.; Yu, L.-Y.; Gao, Z.-P.; Si, S.-Y. A new benzamide derivative from rice fermentation of *Streptomyces* sp. CPCC 202950. *China J. Chin. Materia Med.* **2017**, *42*, 2097–2101.
29. Biggins, J.B.; Liu, X.F.; Feng, Z.Y.; Brady, S.F. Metabolites from the induced expression of cryptic single operons found in the genome of *Burkholderia pseudomallei*. *J. Am. Chem. Soc.* **2011**, *133*, 1638–1641. [[CrossRef](#)]
30. Deng, J.J.; Lu, C.H.; Li, S.R.; Hao, H.L.; Li, Z.U.; Zhu, J.; Li, Y.Y.; Shen, Y.M. p-Terphenyl O- $\beta$ -glucuronides, DNA topoisomerase inhibitors from *Streptomyces* sp. LZ35 $\Delta$ gdmAI. *Bioorganic Med. Chem. Lett.* **2014**, *24*, 1362–1365. [[CrossRef](#)]
31. Han, B.; Li, W.X.; Cui, C.B. Pteridic acid hydrate and pteridic acid C produced by *Streptomyces pseudoverticillus* YN17707 induce cell cycle arrest. *Chin. J. Nat. Med.* **2015**, *13*, 467–470. [[PubMed](#)]
32. Ritzau, M.; Heinze, S.; Fleck, W.F.; Dahse, H.M.; Graefe, U. New macrodiolide antibiotics, 11-O-monomethyl- and 11,11'-O-dimethylelaiophylins, from *Streptomyces* sp. HKI-0113 and HKI-0114. *J. Nat. Prod.* **1998**, *61*, 1337–1339. [[CrossRef](#)] [[PubMed](#)]
33. Xin, W.X.; Ye, X.W.; Yu, S.R.; Lian, X.Y.; Zhang, Z.Z. New capoamycin-type antibiotics and polyene acids from marine *Streptomyces fradiae* PTZ0025. *Mar. Drugs* **2012**, *10*, 2388–2402. [[CrossRef](#)] [[PubMed](#)]
34. Ye, X.W.; Anjum, K.; Song, T.F.; Wang, W.L.; Yu, S.R.; Huang, H.C.; Lian, X.Y.; Zhang, Z.Z. A new curvularin glycoside and its cytotoxic and antibacterial analogues from marine actinomycete *Pseudonocardia* sp. HS7. *Nat. Prod. Res.* **2016**, *30*, 1156–1161. [[CrossRef](#)] [[PubMed](#)]